

# Beta Strength Distribution in Neutron - Deficient Nuclei

Z. Janas<sup>a</sup>, J. Agramunt<sup>b</sup>, A. Algora<sup>b</sup>, L. Batist<sup>c</sup>, B.A. Brown<sup>d</sup>,  
D. Cano-Ott<sup>b</sup>, R. Collatz<sup>e</sup>, A. Gadea<sup>b</sup>, M. Gierlik<sup>a</sup>, M. Górska<sup>e,a</sup>,  
H. Grawe<sup>e</sup>, A. Gulielmetti<sup>e</sup>, M. Hellström<sup>e</sup>, Z. Hu<sup>e</sup>, M. Karny<sup>a</sup>,  
R. Kirchner<sup>e</sup>, F. Moroz<sup>c</sup>, A. Piechaczek<sup>f</sup>, A. Płochocki<sup>a</sup>,  
M. Rejmund<sup>e,a</sup>, E. Roeckl<sup>e</sup>, B. Rubio<sup>b</sup>, K. Rykaczewski<sup>g,a</sup>,  
M. Shibata<sup>e</sup>, J. Szerypo<sup>a</sup>, J.L. Tain<sup>b</sup>, V. Wittmann<sup>c</sup>, A. Wöhr<sup>f</sup>

<sup>a</sup>*Institute of Experimental Physics, University of Warsaw, PL-00681 Warsaw, Poland*

<sup>b</sup>*Instituto de Física Corpuscular, C.S.I.C.-Univ. Valencia, E-46100 Burjassot, Spain*

<sup>c</sup>*St. Petersburg Nuclear Physics Institute, 188-350 Gatchina, Russia*

<sup>d</sup>*NSCL, Department of Physics and Astronomy, MSU, East Lansing, MI 48824-1321, USA*

<sup>e</sup>*Gesellschaft für Schwerionenforschung mbH, D-64291, Darmstadt, Germany*

<sup>f</sup>*Instituut voor Kern- en Stralingsfysica, University of Leuven, B-3001 Leuven, Belgium*

<sup>g</sup>*Oak Ridge National Laboratory, Physics Division, PO Box 2008, Oak Ridge, TN 37831, USA*

**Abstract.** The results of recent studies of the Gamow-Teller  $\beta$ -decays of nuclei in the  $^{100}\text{Sn}$  region are presented. Measurements performed with the use of the total absorption  $\gamma$ -ray spectrometer and the Cluster Cube array of germanium detectors revealed qualitatively new information on the Gamow-Teller strength distribution in the decays of  $^{97}\text{Ag}$  and  $^{103-107}\text{In}$ . The shape of the measured  $\beta$ -strength distribution and the resulting total  $B_{GT}$  values are compared with the results of shell-model calculations.

## Introduction

Understanding and reliable description of the  $\beta$ -strength distribution is of crucial importance for the complete characteristics of the nuclear  $\beta$ -decay. The  $\beta$ -strength function determines the gross properties of the decaying nuclei such as half-life or probability of  $\beta$ -delayed particle emission. Predictions and investigations of these basic characteristics of  $\beta$ -unstable nuclei are of primary interest in the decay studies far from stability. Data resulting from these studies provide an important nuclear physics input for the understanding of the element synthesis in the universe. The knowledge of the weak interaction rates in stellar matter evolution, in particular rates of the Gamow-Teller (GT) transitions for iron region nuclei, is crucial for the calculations of the electron capture (EC) rates during the presupernova core collapse of the massive stars [1]. High-precision measurements of superallowed  $0^+ \rightarrow 0^+$  Fermi  $\beta$ -transitions rates allow one to verify the conserved vector current (CVC) hypothesis, to test the unitarity of the Kobayashi-Maskawa matrix and finally to set limits on extensions to the Standard Model [2]. Very sensitive probes

for studying fundamental symmetries of electroweak interaction and properties of neutrino provide studies of double  $\beta$ -decay ( $2\beta$ ) [3]. Reliable calculation of nuclear  $2\beta$ -decay matrix elements is prerequisite for deduction of the neutrino mass from  $2\beta$ -decay experiments. Matrix elements of the GT transitions are needed for the determination of the neutrino capture cross-section for (solar) neutrino detectors [4,5].

In this contribution we restrict our discussion to one of the most intriguing problems related to the  $\beta$ -strength distribution studies which concerns the question of the origin of the quenching observed for the strength of GT transitions. As it is shown by the analysis of the GT  $\beta$ -decays, the experimentally determined strengths appear to be systematically smaller than the calculated GT  $\beta$ -transition rates. Similar regularity is observed for the GT strengths extracted from the forward-angle intermediate-energy charge-exchange reactions [6,7].

The GT quenching can be quantitatively described in terms of the hindrance factor defined as the ratio of calculated and experimentally determined GT strength. The best description of nuclear wave functions and the GT matrix elements between nuclear states is provided by large-basis shell model calculations. The most complete calculations, based on the diagonalization of the effective hamiltonian within the full major oscillator shell, are feasible only for relatively light nuclei. Such calculations were used to determine hindrance factors for nuclei with  $A \leq 50$ . A comparison of the GT decay rates measured and calculated within the full  $p$ -shell for  $A \leq 18$  nuclei revealed the quenching of the observed  $B_{GT}$  values by a factor of 1.49(3) [8]. The systematic analysis of GT strength for  $A=17-39$  nuclei yielded the hindrance factor of 1.68(4) with respect to the complete  $sd$ -shell calculations [9]. The recent analysis of the GT decays in the mass range  $A=41-50$  indicated that the agreement between the experimental data and the full  $fp$ -shell calculations demands the introduction of the average hindrance factor  $h = 1.81(4)$  [10].

Two physically different mechanisms are usually considered to explain the observed quenching of the GT strength. The first one is a renormalization of the axial-vector coupling constant  $g_A$  in nuclear matter originating from non-nucleonic effects mediated mainly by the admixture of the  $\Delta(1232)$ -isobar nucleon-hole configurations to the GT states. The second mechanism responsible for the reduction of the observed GT strength is the higher-order nuclear configuration mixing arising from tensor correlations between nucleons. A recent estimate has shown that two thirds of the amplitude of the GT quenching originates from higher-order nuclear configuration mixing and one third from  $\Delta$ -isobar admixtures [11]. A decisive experimental verification of this conjecture is, however, still lacking. In particular the role of the  $\Delta$  particles contribution continues to be under discussion.

The question of the "missing" GT strength can be adequately addressed in  $\beta$ -decay studies of nuclei far from stability where the GT strength distribution can be investigated and confronted with theoretical predictions over a broad range of excitation energies. In this respect the  $^{100}\text{Sn}$  region is of particular interest: Since the  $N=Z=50$  shell closure occurs far from stability, isotopes in this region, especially non even-even ones, have relatively large  $Q_\beta$ -values. From simple single-particle model considerations one may expect that a substantial part of the total GT-strength resides within the  $Q_{EC}$  window and may thus be detected in  $\beta$ -decay measurements conducted with the proper experimental technique. As far as theo-

retical calculations are concerned, nuclei close to  $^{100}\text{Sn}$  can be treated as closed-shell systems with a few valence particles only, which facilitates the model description.

## GT strength distribution from $\beta$ -decay measurements

The strength of the GT  $\beta$ -transition to the state at excitation energy  $E$  in the daughter nucleus can be derived from the measurements of the  $\beta$  feeding of this state  $I(E)$ , the decay energy  $Q_{EC}$  and the  $\beta$ -decay half-life  $T_{1/2}$  according to the relation:

$$B_{GT}(E) = \frac{D \cdot I(E)}{(g_A/g_V)^2 \cdot f(Q_{EC} - E) \cdot T_{1/2}} \quad (1)$$

where  $D=6147(7)$  s is a constant,  $g_A/g_V=-1.262(4)$  is the ratio of axial-vector and vector coupling constants for the free-neutron decay and  $f$  is the statistical rate function.

Most frequently,  $\beta$ -feeding distribution has been derived from the detailed decay scheme established in conventional measurements employing standard-size Ge detectors. Such studies can often reveal a wealth of nuclear structure data on all individual levels in simple decay schemes and disclose information about the structure of low-lying states in complex decays. For complex decay schemes with high decay energy, however, such traditional measurements are generally unable, due to the low efficiency of detectors, to record all of the many weak  $\gamma$  transitions and hence to place them in the decay scheme. This is particularly true for energetic  $\gamma$ -rays depopulating states at high excitation energy in the decay product. As a consequence, the classical high-resolution  $\gamma$ -ray spectroscopy studies based on routinely applied Ge detectors usually overestimate the  $\beta$ -feeding intensity to low-lying states. Due to the very strong dependence of the  $\beta$ -decay rate function on the transition energy ( $f \sim (Q_{EC} - E)^5$ ), the distortion of the  $\beta$ -feeding distribution has severe impact on the resulting  $B_{GT}$  distribution and causes underestimation of the apparent total GT strength.

A way to overcome the limitations of the standard discrete, high-resolution, low-efficiency  $\gamma$ -ray spectroscopy is a direct measurement of the distribution of  $\beta$ -decay feeding intensity. The ideal tool for this kind of measurements would be a  $\gamma$ -energy calorimeter with 100% full-energy peak efficiency for all  $\gamma$ -ray energies. In such a detector all members of each  $\gamma$  cascade depopulating an excited state would be summed to yield an output signal corresponding to the excitation energy of this state and provide an unambiguous signature for each  $\beta$ -feeding event to the given level.

Today the closest approach to such an ideal spectrometer represents an array of large scintillation detectors in a  $4\pi$  geometry. The total absorption spectrometer (TAS) installed at the on-line mass separator at GSI consists of a large NaI crystal ( $\varnothing 14'' \times 14''$ ) for the detection of  $\gamma$ -rays [12]. A cylindrical well along the crystal's symmetry axis accommodates an assembly of auxiliary detectors. In the standard set-up it contains two Si counters for  $\beta$  particle detection, a high-resolution Ge X-ray detector and a "plug" NaI detector which restores the  $4\pi$  geometry of the main crystal. The tape transport system is used to position mass separated radioactive

sources in the center of the main crystal, between the two Si counters. By demanding coincidence with signals from the Si detectors, the positron component of the  $\beta^+$ /EC decay can be selected, whereas coincidences with characteristic X-rays recorded by the Ge detector can be used to select the EC events. The total  $\gamma$ -ray efficiency of TAS for monoenergetic photons in the energy range of 0.2 - 4.0 MeV exceeds 88%, and its full-energy peak efficiency is above 56%. The high efficiency values and their weak dependence on photon energy assure the operation of the detector as a satisfactory total absorption spectrometer. However, due to the apparent  $\gamma$ -efficiency loss effects, the determination of the  $\beta$ -feeding distribution from the experimental TAS spectra requires thorough knowledge of the detector response function and application of sophisticated deconvolution procedures. These problems have been elaborated by M. Karny et al. [13,14] and D. Cano-Ott et al. [15] who pointed to the importance of the high-resolution studies as a source of necessary input data for extracting the  $\beta$ -feeding distribution from the measured TAS spectra.

The genuine requirement for high-quality discrete spectroscopy data triggered the use of state-of-the-art Ge detectors for  $\beta$ -decay studies. In the experiments performed at the GSI on-line mass separator an array of 6 Euroball Cluster Ge detectors arranged to form a cube (Cluster Cube) has been used to complement the TAS measurements. The 42 Ge crystals of this array covered about 65% of the full solid angle with respect to a source positioned at the center of Cluster Cube, and allowed registration of 1.33 MeV  $\gamma$ -rays with a full-energy peak efficiency of about 19% and typical resolution of about 2.8 keV. The sensitivity of the Cluster Cube exceeds by far the sensitivity of any Ge detector set-up used in previous  $\beta$ -decay measurements and makes it indeed an excellent tool for spectroscopy studies of complicated decays. The usefulness of the Cluster Cube detector has been demonstrated in the measurements of  $^{97}\text{Ag}$  and  $^{150}\text{Ho}(2^-)$  decays performed at GSI on-line mass separator. More than 600  $\gamma$  transitions (580 new) depopulating 150 levels were placed in the decay scheme of  $^{97}\text{Ag}$  [16] An even more complex decay scheme has been established for  $^{150}\text{Ho}(2^-)$  [17]. In both cases, the performance of the Cluster Cube pushed the measurements to the limit of the discrete  $\gamma$ -ray spectroscopy method, i.e. up to the excitation energies where deexcitation by statistical  $\gamma$  cascades deexcitation dominates. The comparison of  $\beta$ -feeding distribution for  $^{150}\text{Ho}(2^-)$  determined from the Cluster Cube data and from the TAS measurement clearly illustrates the limitations of the discrete  $\gamma$ -ray spectroscopy technique for the investigation of  $\beta$ -strength function in complex decays. All in all, the high-resolution, discrete spectroscopy should not be considered as an alternative to the total absorption  $\gamma$ -ray studies but rather as a complementary method which, however, is indispensable for the reliable analysis of the TAS spectra and also needed to reveal the fine-structure of the  $\beta$ -strength distribution.

## GT strength distribution for nuclei in the $^{100}\text{Sn}$ region

The GT decays of nuclei in the vicinity of  $^{100}\text{Sn}$  proceeds via transformation of a  $g_{9/2}$  proton into a  $g_{7/2}$  neutron. On the basis of an extreme single-particle model one expects that this transformation will be dominated by the decay of the even-even core with the unpaired particles acting as spectators. In the decays of odd-odd

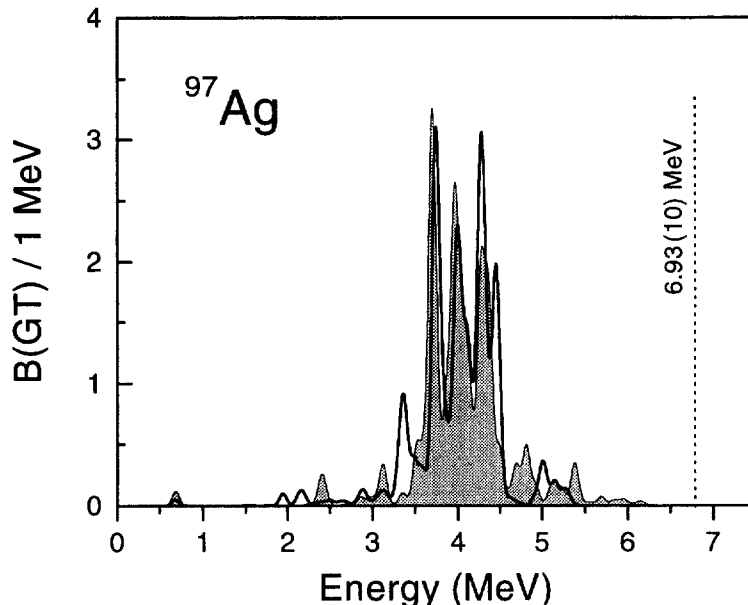


FIGURE 1.  $B_{GT}$  distribution for the decay of  $^{97}\text{Ag}$  deduced from the Cluster Cube measurement (solid line) and obtained from the shell model calculations (shaded area), respectively. Both distributions were smoothed by folding with a Gaussian distribution of 60 keV FWHM. The theoretical data were normalized to the total  $B_{GT}$  value derived from the Cluster Cube measurement. The vertical line indicates the  $Q_{EC}$  value.

isotopes, this corresponds to the dominant population of four-quasiparticle states at excitation energies of 5-6 MeV in the daughter nucleus, whereas in the decays of odd-even nuclei one should observe substantial feeding of three-quasiparticle configurations at an excitation energy of 3-4 MeV. Due to the residual interactions, these configurations are expected to be spread over many levels of the daughter nucleus. Fig. 1 shows the preliminary  $B_{GT}$  distribution for the decay of  $^{97}\text{Ag}$  resulting from the Cluster Cube measurement [16]. The global shape of this distribution is dominated by a resonance structure extending between 3 and 4.5 MeV, in general agreement with the results of the preliminary TAS data analysis [16]. The decay characteristics observed can be interpreted as the GT decay of the even-even core to three-quasiparticle configurations. As shown in Fig. 2, similar structure of the  $B_{GT}$  distribution has been obtained from the TAS measurements for  $^{103-107}\text{In}$ . As expected from the simple single-quasiparticle model, the experimental  $B_{GT}$  distribution is concentrated in resonances appearing at an excitation energy of about 3.5 and 5.5 MeV for odd-mass and even-mass indium isotopes, respectively. The full widths at half maximum of the distributions amount to about 1-1.5 MeV.

More realistic description of the GT strength distribution can be obtained in the shell model approach. Since the conventional shell model calculations within a full major oscillator shell are not feasible due to the very large number of configurations involved, the calculations were performed in the model space designated by SNB in ref. [18], where it was used to calculate  $\beta$ -decay properties of  $N=50$  and  $N=51$  nuclei near  $^{100}\text{Sn}$ . In the full SNB model space the  $1p_{1/2}$  and  $0g_{9/2}$  proton orbitals are active, whereas neutron particles are allowed to occupy  $0g_{7/2}$ ,  $1d_{5/2}$ ,  $1d_{3/2}$ ,

$2s_{1/2}$  and  $0h_{11/2}$  orbitals. In Fig. 1, the GT strength function for  $^{97}\text{Ag}$  resulting from these calculations is confronted with the experimental  $B_{GT}$  distribution. For a comparison of the *shape* of the distributions, the theoretical data displayed in Figs. 1 and 2 were normalized to the total observed  $B_{GT}$  (The hindrance factors with respect to the *absolute*  $B_{GT}$  values will be discussed below). As can be seen from Fig. 1, the SNB calculation fairly well reproduces the position and the fine structure of the GT resonance.

For  $^{103-107}\text{In}$ , the number of the final state configurations was much too large to handle in practical calculations and the SNB model space for neutrons had therefore to be restricted to  $0g_{7/2}$  and  $1d_{5/2}$  orbitals. The results of these calculations are compared to the experimental  $B_{GT}$  distributions in Fig. 2. For all indium isotopes studied in this work, the centroids and widths of the GT resonances are very well reproduced by the shell-model calculations performed in the restricted SNB model space. The shape divergence noticeable in the high-energy part of the  $B_{GT}$  distribution for  $^{103}\text{In}$  most probably indicates the influence of the truncation of the full SNB model space [14].

The GT strength within the SNB model space arises only from the transformation of a  $g_{9/2}$  proton into a  $g_{7/2}$  neutron. The strength of this transition is maximized in  $^{100}\text{Sn}$ , amounting to  $B_{GT}^0=17.78$ . In the general case, the total  $\beta^+$ /EC strength summed over all final states is  $\Sigma B_{GT}=(N_{9/2}/10)\cdot(1-N_{7/2}/8)\cdot B_{GT}^0$ , where  $N_{9/2}$  and

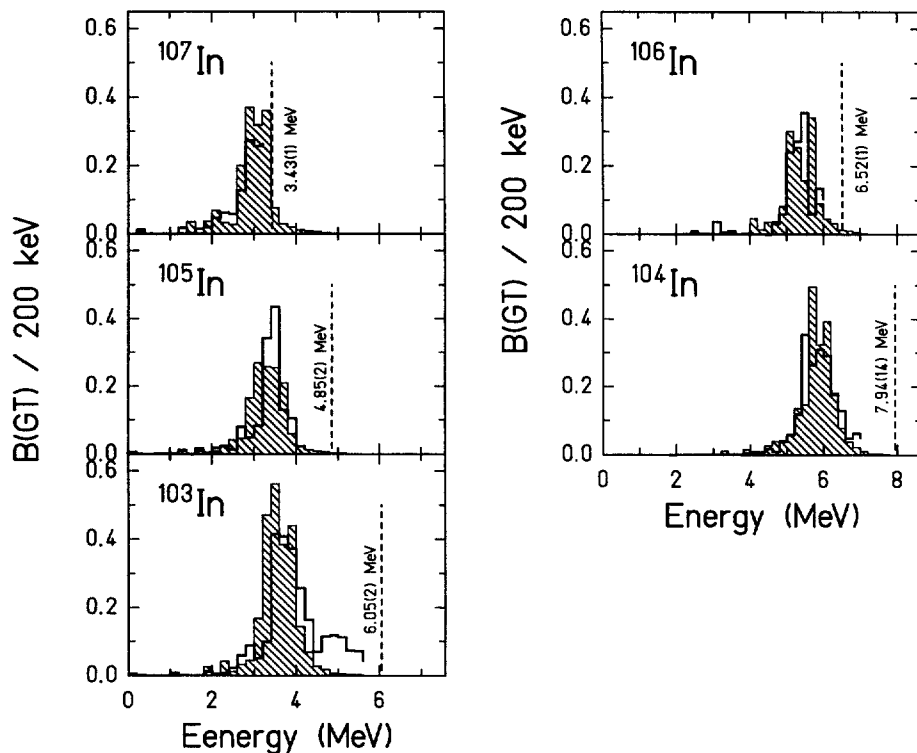


FIGURE 2.  $B_{GT}$  distribution for the decay of neutron-deficient indium isotope derived from the TAS measurements (blank histogram) and resulting from the shell model calculations (hatched histogram). Theoretical distributions were normalized to the total  $B_{GT}$  derived from the TAS measurements. The vertical lines indicate the  $Q_{EC}$  values.

$N_{7/2}$  are the initial state occupancies of the  $\pi g_{9/2}$  and  $\nu g_{7/2}$  orbitals, respectively.

Table 1 summarizes the total  $B_{GT}$  values predicted by the SNB calculations to lay within the  $Q_{EC}$  window and the  $\Sigma B_{GT}$  resulting from the TAS measurements. By comparing the theoretical and experimental  $\Sigma B_{GT}$  values the hindrance factors ranging from 5 to 8 were deduced indicating the importance of the  $0\hbar\omega$  excitations beyond the SNB model space.

TABLE 1. Calculated and experimental  $\Sigma B_{GT}$  for isotopes studied by using the TAS. The respective half-lives ( $T_{1/2}$ ), decay energies ( $Q_{EC}$ ) and hindrance factors ( $h$ ) are also given.

Nucleus	$T_{1/2}(\text{m})$	$Q_{EC}(\text{MeV})$	$\Sigma B_{GT}^{\text{th}}$	$\Sigma B_{GT}^{\text{exp}}$	$h$
$^{97}\text{Ag}$	0.422(5)	6.93(10)	12.8	2.63(37)	4.9(7)
$^{103}\text{In}$	1.08(2)	6.05(2)	12.7	2.47(25)	5.1(5)
$^{104}\text{In}$	1.80(3)	7.91(14)	12.6	2.04(14)	6.2(4)
$^{105}\text{In}$	5.07(7)	4.85(2)	10.9	$1.4_{-3}^{+6}$	$7.8_{-1.7}^{+3.3}$
$^{106}\text{In}$	6.2(1)	6.52(1)	10.7	1.43(8)	7.5(4)
$^{107}\text{In}$	32.4(3)	3.43(1)	8.0	$1.15_{-20}^{+30}$	$6.9_{-1.2}^{+1.8}$

## Summary and conclusions

Measurements performed with the use of the TAS and the array of Euroball Cluster detectors have provided qualitatively new data on the GT strength distribution for nuclei near  $^{100}\text{Sn}$ . For the first time, the complete  $\beta$ -strength in the domain of GT resonance has been mapped for such nuclei. The results obtained constitute a solid basis for a detailed comparison with theoretical predictions. The shell model calculations performed in the SNB model space fairly well reproduce the shape of the measured GT strength distributions. However, the total experimental GT strength was found to be a factor of 5 to 8 smaller than the shell model prediction. This discrepancy can be reduced if one assumes a universal character of the hindrance mechanisms observed in  $p$ -,  $sd$ - and  $pf$ -shells and adopts for the  $^{100}\text{Sn}$  region the global hindrance factor of 1.81, which was introduced to account for the higher-order effects in the  $pf$ -shell. The possible source of the remaining disagreement must then be related to the truncation of the shell model configuration space. In fact, the importance of the intrashell configuration mixing has been demonstrated by the recent shell model Monte Carlo (SMMC) calculations performed for  $^{94}\text{Ru}$ ,  $^{96}\text{Pd}$ ,  $^{96,98}\text{Cd}$  and  $^{100}\text{Sn}$  within the complete  $g$ - $d$ - $s$  oscillator shell [19]. In particular, for  $^{98}\text{Cd}$  the calculations in the SNB model space yield a free-nucleon value of 13.3 for the total  $B_{GT}$  [18], whereas the corresponding  $\Sigma B_{GT}$  obtained in the full  $0\hbar\omega$  calculations amounts to 7.0 [19]. The latter value, when renormalized by the global hindrance factor of 1/1.81, is in excellent agreement with the experimental estimate of  $\Sigma B_{GT}$  equal  $3.5_{-0.6}^{+0.7}$  [20]. It is worth noting that  $^{98}\text{Cd}$  is the nucleus closest to  $^{100}\text{Sn}$  for which the experimental  $B_{GT}$  can be confronted with the results of the complete  $0\hbar\omega$  calculations. However, for the critical test of the theory, the extension of the SMMC calculations to non even-even iso-

topes in the vicinity of  $^{100}\text{Sn}$ , for which reliable GT strength distributions have been determined from TAS measurements, is highly desirable.

Future experimental studies of GT decays should approach nuclei as close to  $^{100}\text{Sn}$  as possible with the ultimate goal to measure the complete distribution of the GT strength of  $^{100}\text{Sn}$  itself in a reliable manner, i. e. to improve the scarce data available for this decay. For the case of  $^{102}\text{In}$  the TAS and Cluster Cube data are being analysed. Measurements for  $^{100}\text{In}$  and  $^{101}\text{In}$  decays are planned, and the reinvestigation of  $^{98}\text{Cd}$  decay by means of the total absorption technique is considered. For the most exotic nuclei the  $\gamma$ -ray measurements have to be complemented by the investigation of  $\beta$ -delayed particle emission.

## Acknowledgments

This work was supported in part by the Polish Committee of Scientific Research under grant KBN 2 P03B 039 13, by the Russian Fund for Basic Research and Deutsche Forschungsgemeinschaft under contract No. 436 RUS 113/201/0(R), by the U.S. N.S.F. under grant 9605207, by C.I.C.Y.T. (Spain) under project AEN96-1662, and by the EC Contract No. ERBFMGECT950083. M.K. would like to acknowledge financial support from the Foundation for Polish Science. B.A.B. wishes to thank the A. von Humoldt Foundation for support. K.R. would like to thank for a partial support from the U.S. D.O.E. under project DE-AC05-96OR22464 and ORNL managed by Lockheed Martin Energy Research Corporation.

## References

1. Bethe, H.A., *Rev. Mod. Phys.* **64**, 491 (1992).
2. Hardy, J.C., Towner, I.S., *contribution to this conference*.
3. Ejiri, H., *Acta Physica Polonica* **B29** 47 (1998).
4. Trinder, W., et al., *Phys. Lett.* **B349**, 267 (1995).
5. Liu, W., et al., *Z. Phys.* **A386**, 1 (1997).
6. Osterfeld, F., *Rev. of Mod. Phys.* **64**, 491 (1992).
7. Koonin, S.E., et al., *Annu. Rev. Nucl. Part. Sci.* **47**, 463 (1997).
8. Chou, W.T., Warburton, E.K., Brown, B.A., *Phys. Rev.* **C47**, 163 (1993).
9. Brown, B.A., Wildenthal, B.H., *At. Data Nucl. Data Tables* **33**, 348 (1985).
10. Martínez-Pinedo, G., et al., *Phys. Rev.* **C53**, R2602 (1996).
11. Brown, B.A., *Annu. Rev. Nucl. Part. Sci.* **38**, 38 (1988).
12. Karny, M., et al., *Nucl. Instr. and Meth. Phys. Res.* **B126**, 320 (1997).
13. Karny, M., et al., *contribution to this conference*.
14. Karny, M., et al., *Nucl. Phys. A*, in print.
15. Cano-Ott, D., et al., *contribution to this conference*.
16. Hu, Z., et al., *contribution to this conference*.
17. Agramunt, J., et al., *contribution to this conference*.
18. Brown, B.A., Rykaczewski, K., *Phys. Rev.* **C50**, 2270 (1994).
19. Dean, D.J., et al., *Phys. Lett.*, **B367**, 17 (1996).
20. Płochocki, A., et al., *Z. Phys.*, **A342**, 43 (1992).